PNIPAAm-Grafted-Collagen as an Injectable, In Situ Gelling, Bioactive Cell Delivery Scaffold

Scott D. Fitzpatrick,[†] M. A. Jafar Mazumder,[‡] Frances Lasowski,[†] Lindsay E. Fitzpatrick,[‡] and Heather Sheardown*[,†,‡]

School of Biomedical Engineering and Department of Chemical Engineering, McMaster University, 1280 Main Street West, Hamilton ON, L8S 4L7

Received March 18, 2010; Revised Manuscript Received July 14, 2010

We synthesized two thermoresponsive, bioactive cell scaffolds by decorating the backbone of type I bovine collagen with linear chains of poly(*N*-isopropylacrylamide) (PNIPAAm), with the ultimate aim of providing facile delivery via injection and support of retinal pigment epithelial (RPE) cells into the back of the eye for the treatment of retinal degenerative diseases. Both scaffolds displayed rapid, subphysiological phase transition temperatures and were capable of noninvasively delivering a liquid suspension of cells that gels in situ forming a cell-loaded scaffold, theoretically isolating treatment to the injection site. RPE cells demonstrated excellent viability when cultured with the scaffolds, and expulsion of cells arising from temperature-induced PNIPAAm chain collapse was overcome by incorporating a room-temperature incubation period prior to scaffold phase transition. These results indicate the potential of using PNIPAAm-grafted-collagen as a vehicle for the delivery of therapeutic cells to the subretinal space.

Introduction

Cell-based therapies have the potential to provide cures for a vast array of diseases and disorders, especially with the rapid advancement in stem cell technology. However, one of the major obstacles standing in the way of clinical success of cell-based therapies is the development of appropriate vehicles to deliver therapeutic cells to target tissues within the body. Typically, cells are delivered as a liquid suspension injected directly into target tissues or into the systemic circulation.[1] The cells are then expected to migrate to the site of interest or remain within target tissues depending on the delivery modality. Very little in the way of guidance cues is provided to transplanted cells, and the result is typically large-scale cell death, mass leakage of cells from target tissues, loss of control over transplanted cell fate, and extremely poor integration into host tissues, often with <3% of cells remaining in the intended tissue.[1] Alternatively, cells can be seeded, expanded, and differentiated on or within a biomaterial scaffold ex vivo and subsequently implanted at a target location within the body. Delivering cells within a scaffold addresses many of the issues associated with bolus injections by providing a synthetic ECM for cell adhesion, preventing anoikis, and isolating cells to the implantation site. Furthermore, it is possible to load cell scaffolds with growth factors or pharmaceuticals, which help control cell phenotype and modulate the microenvironment at the site of implantation.[2] However, implantation of scaffolds is inherently more invasive than bolus cell delivery, which is achieved by simple injection.

Retinal degenerative diseases are a family of diseases that stand to benefit greatly from recent advances in cell technology as researchers have recently demonstrated the potential to prevent or reverse vision loss using cell therapy. MacLaren et al. demonstrated the possibility of repopulating a damaged or diseased retina with healthy photoreceptors through delivery of neonatal photoreceptor precursor cells; the cells differentiated and integrated with limited success into the outer nuclear layer (ONL) in both intact and degenerating retinas of mature mice.[3] Delivery of retinal pigment epithelial (RPE) cells is another cell-based therapy that has demonstrated tremendous potential and has seen exciting developments since its first inception over 20 years ago.[4−7] RPE transplantation aims to restore the dynamic interaction between light sensitive photoreceptors and metabolically active RPE cells, a relationship that is critical for the maintenance of retinal homeostasis and preservation of sight.[8] Restoration of the subretinal anatomy and extracellular milieu through RPE transplantation can be used to treat not only RPE specific defects but also a number of photoreceptor defects as well as more complex retinal diseases such as age-related macular degeneration (AMD).[9] Delivery of therapeutic cells into the subretinal space with an appropriate scaffold may help ease the transition from implantation to integration and improve outcomes with retinal cells.[9,10] Subretinally transplanted photoreceptors may also benefit from delivery within a temporary scaffold; however, the need to integrate into retinal tissues requires migration out of the scaffold and into the retina. Therefore, an appropriate scaffold should be short-lived and promote localized treatment while providing temporary adhesive cues and ultimately may serve best as a template for the controlled release of a symphony of growth factors to aid the migration and differentiation of transplanted cells.[2] Alternatively, anchorage-dependent RPE cells, which need not migrate from the subretinal space, may benefit greatly from delivery within a relatively long-lasting artificial scaffold that provides enhanced cellular attachment. A temporary scaffold would localize transplanted cells to the subretinal space and allow cells to lay down their own extracellular matrix (ECM). This may aid their eventual adhesion to the native subretinal basement membrane, the Bruch's membrane, which may be compromised because of age- or disease-related structural changes.[10]

Notwithstanding the above, delivery of therapeutic cells into the complex subretinal space is a particularly challenging task,

* To whom correspondence should be addressed. E-mail: sheardow@mcmaster.ca.
[†] School of Biomedical Engineering.
[‡] Department of Chemical Engineering.

10.1021/bm100299j
Published on Web 08/09/2010

and typical delivery modalities have resulted in poor integration and limited functioning of transplanted cells in the clinical setting.[9] Bolus cell injections are inefficient, resulting in mass efflux of cells into the vitreal cavity and the formation of island-like cell aggregates, whereas RPE patch grafts require invasive surgical implantation through a small incision made in the retina, which may damage the highly complex neural retinal tissues.[8,9] It is likely that minimally invasive cell delivery techniques are crucial for the clinical success of retinal cell-based therapy. Therefore, it was hypothesized that the development of cell-carrying "intelligent materials", delivered through relatively noninvasive methods and which can be tailored to provide short and long-term support as required, may serve as ideal delivery vehicles for transplantation and support of therapeutic cells into the subretinal space and ultimately other tissues.

Intelligent materials undergo a reversible, stimuli-induced phase transition that can be utilized to deliver therapeutic agents noninvasively via syringe as a liquid suspension, followed by scaffold formation in situ and subsequent entrapment of the delivered agent.[11] Poly(*N*-isopropylacrylamide) (PNIPAAm) is a thermoresponsive intelligent material that undergoes a reversible transition from liquid to gel under aqueous conditions when heated above a lower critical solution temperature (LCST) of ~32 °C.[11] It was envisioned that the rapid phase transition, characteristic of PNIPAAm, could be utilized to deliver cells as a liquid suspension to the subretinal space, followed by in situ scaffold formation, in essence combining the favorable delivery technique of bolus injections with the benefits of providing transplanted cells with a synthetic ECM for support. PNIPAAm has been used in a number of different biomedical applications. For example, Hoffman et al. developed PNIPAAm−protein conjugates to modulate temperature-induced on−off biochemical activity for use in immunoassays and protein isolation.[12,13] Additionally, the polymer has been examined extensively for use in drug delivery systems[14,15] and in "cell sheet engineering" to generate an intact monolayer of functional cells without the use of digestive enzymes.[16] Cells harvested in this fashion have been examined for transplantation as single sheets for skin,[19] cornea,[18] and RPE[8] repair, or as more complex layered sheets for cardiac,[16] kidney,[17] and liver[20] tissue regeneration. However, because PNIPAAm contains no cell-binding domains in its unmodified form, it does not serve as an appropriate template for transplanted cell adhesion. Therefore, to generate an injectable, in situ gelling, cell adhesive scaffold, PNIPAAm must be coupled to adhesion molecules or peptide sequences that support anchorage of the transplanted cells. RPE cells adhere to their ECM, neighboring cells, and Bruch's membrane through a number of different adhesion molecules including integrins, cadherins, syndecans, selectins, and immunoglobulin adhesion proteins.[9] Of these adhesion molecules, the integrins are of significant interest because they play an essential role in the adhesive and phagocytic activity of RPE cells, which is crucial for the maintenance of retinal homeostasis and the preservation of sight.[9,17,18] The RPEs appear to have major membrane receptors for collagen, vitronectin, laminin, and fibronectin.[17,19] Therefore, to generate an appropriate substitute for the native Bruch's membrane, in this work, PNIPAAm was coupled to type I collagen, a naturally occurring cell-matrix protein that serves as one of the major binding proteins for RPE cells.[9] The resulting thermoresponsive PNIPAAm−collagen copolymers were examined as cell-carrying biomaterial scaffolds aimed at improving outcomes in retinal-cell therapy for the treatment of retinal degenerative diseases.

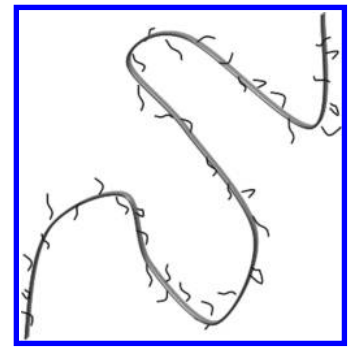

Figure 1. Representative cartoon depicting the presumed structure of the PCol and UV PCol scaffolds in which linear chains of amine-terminated PNIPAAm have been decorated along the backbone of type I bovine collagen, producing a comb-type grafting architecture.

Materials and Methods

Unless otherwise stated, all reagents were purchased from Sigma Aldrich (Oakville, ON).

Synthesis of Amine-Terminated PNIPAAm. *N*-isopropylacrylamide (NIPAAm) was purified by recrystallization from a toluene/hexane mixture. Amine-terminated PNIPAAm was synthesized as described in the literature.[20] In brief, NIPAAm (88.37 mmol) and cysteamine hydrochloride (AESH) (3.68 mmol) were dissolved in dimethylformamide (DMF). Dry nitrogen was bubbled through the reaction mixture for 30 min prior to the addition of *N*,*N*′-azobisisobutyronitrile (AIBN) (1.22 mmol), which had previously been recrystallized from methanol. Polymerization was allowed to proceed for 7 h at 70 °C. The polymerized product was precipitated in an excess of diethyl ether. The product was extensively dialyzed with cellulose tubing (Spectrum Laboratories), then freeze-dried and stored at −20 °C. Both DMF and tetrahydrofuran (THF) gel permeation chromatography (GPC) were used to assess the molecular weight of the polymer using poly(ethylene oxide) (PEO) and polystyrene (PS) standards respectively.

Synthesis of PNIPAAm-Grafted-Collagen. Linear chains of amine-terminated PNIPAAm were grafted onto the backbone of type I bovine collagen (a kind gift of Allergan, Santa Barbara CA) using 1-ethyl-(3-3-dimethylaminopropyl) carbodimiide hydrochloride (EDC) and *N*-hydroxysuccinimide (NHS) chemistry. The cartoon in Figure 1 illustrates the proposed structure of the comb-type graft copolymer. EDC/NHS chemistry was used to generate covalent linkages between the carboxylic acid groups of aspartic acid (Asp) and glutamic acid (Glu) residues present in collagen with the amine-functionalized end groups of the synthesized PNIPAAm.[21] Collagen (0.5 mL, 100 mg/mL) was acidified by thoroughly mixing with HCl (75 μL, 1 N). Amine-terminated PNIPAAm (600 mg) was dissolved in PBS (10 mL, pH 7.2) and was mixed vigorously with the acidified collagen. EDC and NHS (5/5/1 molar ratio of EDC/NHS/collagen COOH groups) were added to the mixture, and the pH was adjusted to 5.5 with HCl. The reaction was allowed to proceed under gentle mixing at room temperature for 24 h. The reaction mixture was dialyzed extensively at 4 °C to remove any EDC, NHS, and excess PNIPAAm. The final copolymer, designated PCol, was freeze-dried and stored at −20 °C.

Alternatively, grafting of amine-terminated PNIPAAm onto a collagen backbone was achieved via UV photo-cross-linking, with the resulting copolymer designated UV PCol. Riboflavin was used as a photosensitizer to generate covalent linkages between PNIPAAm and collagen. Collagen (0.5 mL, 100 mg/mL) was acidified by thoroughly mixing with HCl (75 μL, 1 N). PNIPAAm (100 mg) was dissolved in PBS (5 mL, pH 7.2) and mixed with collagen. The pH was adjusted to 5.5 with HCl. The riboflavin photosensitizer (1 mg/mL in PBS) was added to the mixture at a volume ratio of 1:20 photoinitiator/collagen solution. The final mixture was placed in a UV oven for 15 min, 365 nm, 12.5 W/cm^2. The resulting copolymer was dialyzed extensively at 4 °C, freeze-dried, and stored at −20 °C.

Grafting of PNIPAAm chains onto the collagen backbone via EDC/NHS chemistry and by UV photo-cross-linking was confirmed using Fourier transform infrared spectroscopy (FTIR) (Nicolet-6700, Thermo Scientific). Samples were prepared in a 12:1 PNIPAAm-to-collagen ratio, and unbound chains of PNIPAAm were removed from PCol and UV PCol by extensive dialysis using tubing with MWCO of 50 ,000. IR spectra were then collected for collagen, amine-terminated PNIPAAm, and purified PCol and UV PCol.

Phase Transition Characterization. Phase transition properties of amine-terminated PNIPAAm, collagen, PCol, and UV PCol were analyzed using differential scanning calorimetry (DSC) (TA Instruments, 2910) with hermetic pans. Samples were dissolved (15 mg/mL) in deionized water and were stored at 4 °C prior to analysis. Thermal scans were performed from 25 to 80 °C at a rate of 5 °C/min.

A Cary 300 UV/vis spectrophotometer was used to analyze the change in transmittance associated with the phase transition of PNIPAAm, PCol, and UV PCol scaffolds as they transitioned from a relatively clear liquid to a milky white gel. The samples were dissolved in distilled water to a concentration of 1 mg/mL. Samples were placed in 4 mL UV cuvettes and were subjected to a heating rate of 1 °C/min from 25 to 45 °C. Transmittance measurements were recorded every 30 s. To avoid bubble formation during heating, samples were sonicated briefly prior to testing.

We assessed the gelling kinetics of PNIPAAm, PCol, and UV PCol as a function of temperature by placing glass vials containing 3 mL suspensions of the various materials (5 mg/mL in PBS) in an oil bath at temperatures ranging from 34 to 45 °C. The time required for the samples to reach cloud point was recorded.

Cell Culture. Human RPE cells (CRL-2502) were purchased commercially from ATCC (Manassas, VA) and were cultured under CO_2 (37 °C, 5% CO_2, 95% air, 100% humidity). DMEM-F12 culture medium (Gibco) was supplemented with FBS (6.25% final concentration, Gibco), 1× glutamate (1% final concentration, Gibco), penicillin−streptomycin (1% final concentration, Gibco), and sodium bicarbonate (0.8% final concentration, Gibco). Scaffolds were pretreated with a solution of PBS and penicillin−streptomycin (3:1 v/v) to remove biological contaminants. All tests were run in triplicate. We assessed cell viability in 2- and 3-D cultures by staining cultured cells with calcein AM and ethidium homodimer (EthD-1) (Invitrogen) and manually counting the total number of live and dead cells. One-factor analysis of variance (ANOVA) was used to analyze the effect of scaffold type on RPE viability under 2- and 3-D culture conditions using $\alpha = 0.05$. Statistical analysis of means was performed using PASW Statistics 18 (SPSS, Inc., IL). All error bars on graphs represent standard deviation.

2-D Cell Supernatant Assay. RPE cells were seeded at a density of 10 000 cells per well in a 48-well tissue-culture-treated polystyrene (TCPS) dish. Cells were incubated for 2 h to allow seeded cells to adhere to the bottom of the dish. Culture media was replaced with fresh media containing either amine-terminated PNIPAAm, PCol or UV PCol (20 mg/mL). Culture dishes were then returned to the incubator, allowing the PNIPAAm-based scaffolds to gel in the supernatants of the preadhered cells. Media was changed after 48 h, and viability was assessed after 96 h.

3-D Cell Suspension Assay. RPE cells were suspended at a concentration of 100 000 cells per well in suspensions of PCol and UV PCol (20 mg/mL in DMEM-F12). Suspensions were added to a 48-well TCPS plate, then placed in a 37 °C CO_2 incubator, where the scaffolds gelled, entrapping the cells within the 3-D biomaterial matrix. Culture media was changed every 2 to 3 days, and cell viability was assessed at days 4, 7, and 14.

Cellular Entrapment Within the Scaffold. To promote cellular attachment to the collagen backbone and improve entrapment within the scaffolds, we added a room-temperature incubation period prior to temperature-induced scaffold gelation. Suspensions of amine-terminated PNIPAAm, PCol, and UV PCol (5 mg/mL in DMEM-F12) were loaded with 500 000 RPE cells prestained with calcein AM. Cell-loaded scaffolds were incubated at room temperature for 1 h and then placed in a 37 °C CO_2 incubator to drive gelation of the mixture. After 1 h in the incubator, a temperature-controlled, 37 °C Leica DMI 6000 B confocal microscope was used to visualize the distribution of cells within the bulk phase of the scaffolds to assess whether cells remained dispersed within the scaffold or had been expelled with the aqueous phase during temperature-induced condensation of the PNIPAAm chains.

Environmental Scanning Electron Microscopy. High-resolution images of the internal pore structure of amine-terminated PNIPAAm, unmodified collagen, PCol, and UV PCol were obtained using an Electroscan 2020 environmental scanning electron microscope (ESEM). The samples were swollen (15 mg/mL) in distilled water for 48 h at 37 °C and then rapidly frozen by submersion in a liquid nitrogen bath to preserve the internal pore structure of the swollen scaffolds. The samples remained in the liquid nitrogen bath for 48 h and were subsequently freeze-dried for imaging. RPE cells were loaded in a PCol suspension (15 mg/mL in DMEM-F12) and imaged using ESEM with the described preparation techniques.

Results and Discussion

Synthesis of Amine-Terminated PNIPAAm. Polymerization of NIPAAm in the presence of the chain transfer reagent cysteamine hydrochloride (AESH) yielded an amine-functionalized PNIPAAm with a rapid, thermoreversible phase transition from liquid to gel under aqueous conditions at 32 °C. Amine-terminated PNIPAAm was found to have a molecular weight in the range of 5000 to 10 000 Da using both DMF and THF GPC with PEO and PS standards, respectively.

Synthesis of PNIPAAm-Grafted-Collagen. Initially, simple blends of PNIPAAm and collagen were investigated as potential delivery vehicles. However, these blends tended to separate as PNIPAAm underwent a temperature-induced phase transition. Therefore, it was hypothesized that simple blends would not be sufficient for subretinal cell delivery because separation may lead to efflux of the cell-carrying collagen away from the target tissues and into the vitreal cavity. Therefore, it was determined that grafting temperature-sensitive PNIPAAm chains along the cell-adhesive collagen backbone would provide a better cell delivery vehicle for subretinal transplantation. Collagen cross-linking via EDC/NHS chemistry has been shown to yield materials that are nontoxic both in vitro and in vivo.[22] Therefore, this chemistry was used to facilitate grafting of the amine-terminated PNIPAAm chains to carboxylic acid groups of collagen. Ultraviolet-A (UVA) and riboflavin induction of corneal collagen cross-links is a method used in vivo for the treatment of keratoconnus to increase the biomechanical rigidity and stability of the cornea and offered an alternate means to engraft PNIPAAm chains onto a collagen backbone.[23−25] The presence of ∼122 carboxylic acid groups per collagen α-chain provides a high number of potential PNIPAAm grafting sites along the collagen backbone.[21] Through EDC/NHS chemistry and photo-cross-linking, two cell-friendly, presumably comb-type graft copolymers were synthesized that exhibit a sharp phase transition below physiological temperatures. It is hypothesized that these scaffolds will enable the delivery of a liquid suspension of cells that forms a gel scaffold upon injection into the body that will act as an artificial Bruch's membrane capable of supporting the growth and differentiation of anchorage-dependent RPE cells. The cartoon in Figure 1 is an illustration of the presumed comb-type graft architecture achieved by grafting linear chains of PNIPAAm along the length of a collagen backbone.

Unbound PNIPAAm chains were removed from PCol and UV PCol samples through extensive dialysis, and samples were

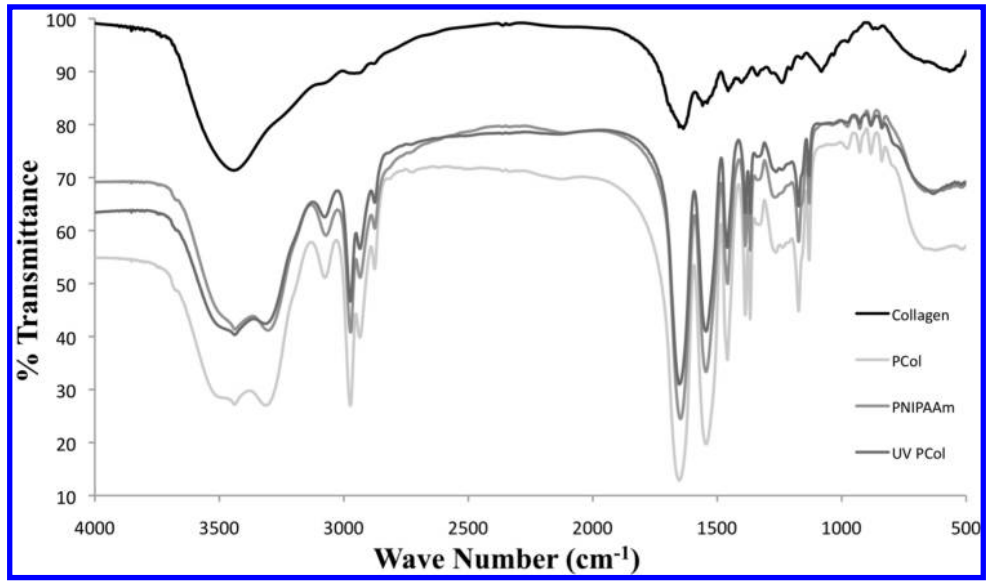

Figure 2. FTIR spectra for collagen, amine-terminated PNIPAAm, and purified PCol and UV PCol. Characteristic PNIPAAm peaks are seen in both PCol and UV PCol samples following the removal of unbound PNIPAAm polymer chains, demonstrating that successful grafting has occurred through EDC/NHS chemistry and UV photo-cross-linking.

analyzed using FTIR. The presence of bound PNIPAAm chains in both samples was confirmed by the occurrence of characteristic PNIPAAm−$CH(CH_3)_2$ asymmetric deformation (vibration) peaks at roughly 1387 and 1367 cm^{-1} (Figure 2). The presence of these peaks in the purified samples confirms that both EDC/NHS chemistry and UV photo-cross-linking were successful in grafting PNIPAAm chains onto the collagen backbone. Further evidence of successful grafting is indicated by the increased intensity of the secondary amide peaks around 1544 cm^{-1} in the spectra.

We are currently working on a number of different techniques to quantify the grafting density of PNIPAAm chains onto the collagen backbone, which will be reported separately along with data on the effect of graft density on the transitions and cellular response.

Phase Transition Characterization. DSC analysis revealed subphysiological phase transition temperatures for amine-terminated PNIPAAm, PCol, and UV PCol, which are essential for in situ gelling systems that are to be delivered noninvasively through a syringe and undergo a temperature-induced phase transition. Multiple peaks were observed for the PCol and UV PCol scaffolds; presumably, the primary peaks resulted from a PNIPAAm-induced phase transition, whereas secondary peaks arose because of denaturation of the collagen backbone. Denaturation of unmodified collagen was observed at 50 °C, similar to our previous studies.[26] As expected, typically, an increase in the thermal transition of collagen was observed following PNIPAAm grafting, although in some cases, clear transitions were not observed, and denaturation appeared to take place over a range of temperatures. However, the apparent increase in collagen denaturation temperature suggests that PNIPAAm grafting and the slight collagen cross-linking that is also expected to occur impart stability into the collagen structure, a finding that was previously reported for EDC/NHS and dendrimer cross-linked collagen by Duan et al.[26]

Turbidity Analysis. As the PNIPAAm-based scaffolds underwent a phase transition, they transformed from a transparent liquid to a milky white, opaque gel. This cloud point allowed characterization of the scaffold LCST with changes in transmittance using a UV spectrophotometer. PNIPAAm, PCol, and UV PCol were dissolved in distilled water to concentrations of 1 mg/mL, and transmittance was measured at temperatures ranging from 25 to 45 °C with a heating rate of 1 °C/min, as shown in Figure 3.

Table 1. Representative Phase Transition Temperatures of the Different Cell Scaffolding Components As Determined via Differential Scanning Calorimetry Using a Heating Rate of 5°C/min

sample	thermal phase transition (°C)	collagen denaturation (°C)
PNIPAAm-NH_2	32	
collagen		50
PCol	32	65−72
UV PCol	31	54−77

Phase transition temperatures obtained via UV spectrophotometry corresponded with the DSC analysis. All samples appeared to undergo rapid gelation at their LCST, as indicated by the sudden decrease in transmittance. Rapid gelation of the scaffold is desirable to minimize the leakage of liquid scaffold and transplanted cells from the site of injection, thereby maximizing therapeutic payload while minimizing complications that may arise because of scaffold leakage.

Rapid gelling kinetics of all samples was confirmed by assessing the time required to reach cloud point when vials containing suspensions of the different materials were immersed

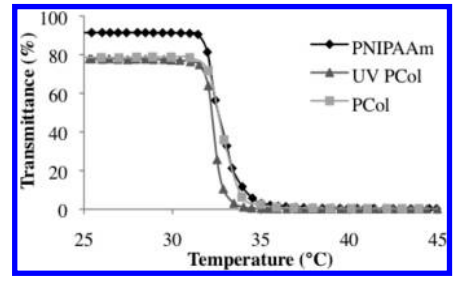

Figure 3. Phase transition analysis of the different PNIPAAm-collagen based scaffold as analyzed by UV spectrophotometry. All samples demonstrated a subphysiological phase transition, which is essential for allowing noninvasive delivery of a liquid suspension of cells that undergo a temperature-induced scaffold formation in situ. Rapid scaffold formation, as indicated by the sudden decrease in transmittance, will promote isolation of therapy to the target, subretinal tissues.

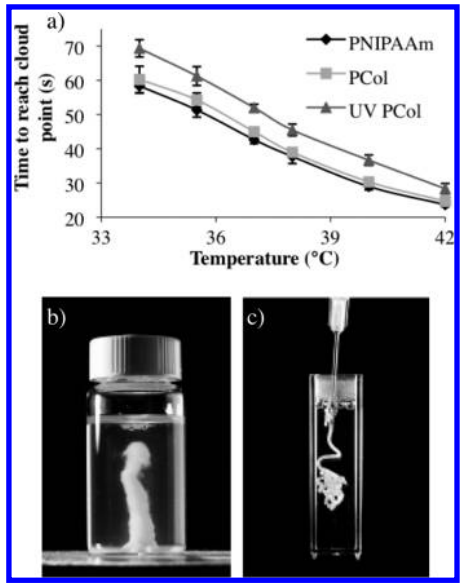

Figure 4. (a) We assessed gelling kinetics of amine-terminated PNIPAAm, PCol, and UV PCol by immersing samples in an oil bath at various temperatures and assessing the time required to reach cloud point under gentle agitation. (b) Gelling times were limited by heat transfer from the oil bath to the solution within the glass vials, as demonstrated by the nonhomogeneous scaffold formation occurring at the bottom of the vial of a PNIPAAm solution being heated on a hot plate. (c) When injected directly into a heated aqueous environment, scaffold formation occurs almost instantaneously. Error bars represent standard deviation.

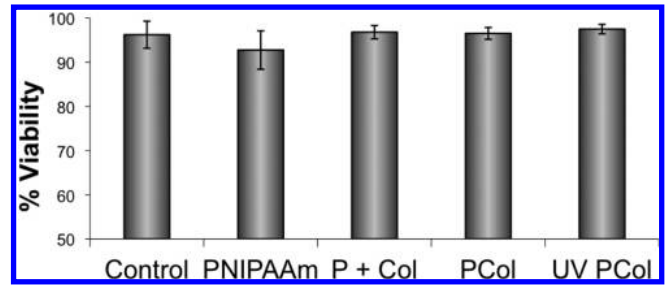

Figure 5. Cell viability of RPE cells when seeded for 96 h in the presence of (a) supplemented DMEM-F12 culture medium, (b) PNIPAAm, (c) PNIPAAm + collagen (P + Col), (d) PCol, and (e) UV PCol. Viabilities were all >90%, and there were no were significant differences between mean viabilities (ANOVA, $p = 0.262$).

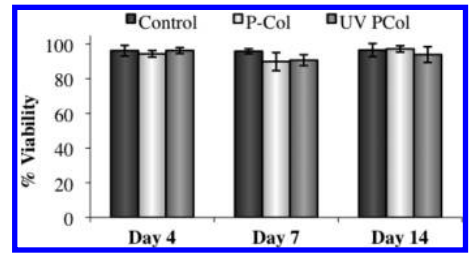

Figure 6. RPE cells demonstrated excellent viability when cultured within the bulk matrix of the PCol and UV PCol scaffolds. TCPS was used as a control. The scaffold type did not significantly affect the mean viability on days 4, 7, and 14 ($p > 0.18$). However, whereas viability remained high, the fraction of cells remaining entrapped within the 3-D architecture was relatively low.

in an oil bath at various temperatures under gentle agitation. Rapid gelling times were observed and were found to decrease as a function of increasing temperature. At physiological temperature, the cloud point was reached in <1 min for all samples. However, gelling kinetics was limited by heat transfer from the oil bath to the samples contained within the glass vials, as illustrated by the slow, nonhomogeneous heating of a representative PNIPAAm solution on a hot plate in Figure 4b. When PNIPAAm, PCol, and UV PCol were injected directly into aqueous solutions above their LCST, scaffold formation occurred almost instantaneously, as demonstrated in Figure 4c with the injection of PNIPAAm into a heated water solution.

The rapid scaffold formation displayed by both synthesized biomaterial scaffolds indicated that cell entrapment should occur promptly upon injection into the subretinal space, providing transplanted RPE cells with a synthetic ECM within which they can adhere. Without an adequate substitute for adhesion, studies have demonstrated that the aged Bruch's membrane may be insufficient for supporting transplanted cell anchorage, differentiation, and survival.[10] As a result, transplanted RPE cells that are unable to attach to an appropriate basement membrane will undergo a process of adhesion-dependent apoptosis, or anoikis.[9] Ideally, cells entrapped within the replacement Bruch's membrane (PCol or UV PCol) will be able to carry out a number of their key functions, such as clearing the subretinal space of debris shed by photoreceptor outer segments, maintenance of the blood-retinal barrier (BRB), and the transport and secretion of various ions, cytokines, and growth factors.[8] However, eventual migration from the scaffold and adhesion to the native Bruch's membrane may be required to carry out these functions. By providing a temporary synthetic scaffold, transplanted cells will be afforded time to lay down their own ECM, which should aid the ultimate attachment to the aged Bruch's membrane. The ideal scaffold lifetime will be elucidated in future studies and will be achieved with the use of a cell-adhesive degradable PNIPAAm, which is currently in development and will theoretically be cleared from the subretinal space following emigration of transplanted cells and material degradation.

Cell Culture. *2-D Cell Supernatant Assay.* Following 96 h of incubation with PNIPAAm, PCol, or UV PCol suspended in the supernatant, RPE cells were stained with calcein AM and EthD-1, and viability was assessed. Viabilities were found to exceed 90% for all conditions (Figure 5), and there were no statistically significant differences among the mean viabilities of the different samples ($p = 0.262$).

3-D Cell Suspension Testing. RPE cells were entrapped within PCol and UV PCol suspensions at a density of 100 000 cells per well and cultured for 4, 7, and 14 days. TCPS was used as a control. Cells were stained with calcein AM and EthD-1 to assess viability. Results are shown in Figure 6.

RPE viability was also high when seeded within the 3-D matrix of the PCol and UV PCol scaffolds. The scaffold type did not significantly affect the mean viability of RPE cells within the scaffolds on days 4, 7, and 14 ($p > 0.18$). However, only a small fraction of the cells originally present in the liquid scaffold remained within the gel following phase transition. The temperature-induced condensation of PNIPAAm chains results in the expulsion of the bulk aqueous phase, which acts as a driving force to expel cells that had not yet adhered to the collagen scaffold.

Successful entrapment and survival of cells within the delivery scaffold is essential for the ultimate success of transplantation because these scaffolds will serve as the replacement substrate for the native Bruch's membrane and must provide temporary support for anchorage-dependent RPE cell attachment while the cells lay down their own ECM. Therefore, it was realized that a change was required to improve the scaffold's ability to entrap transplanted cells successfully and thereby increase the retention of cells when injected into the subretinal space.

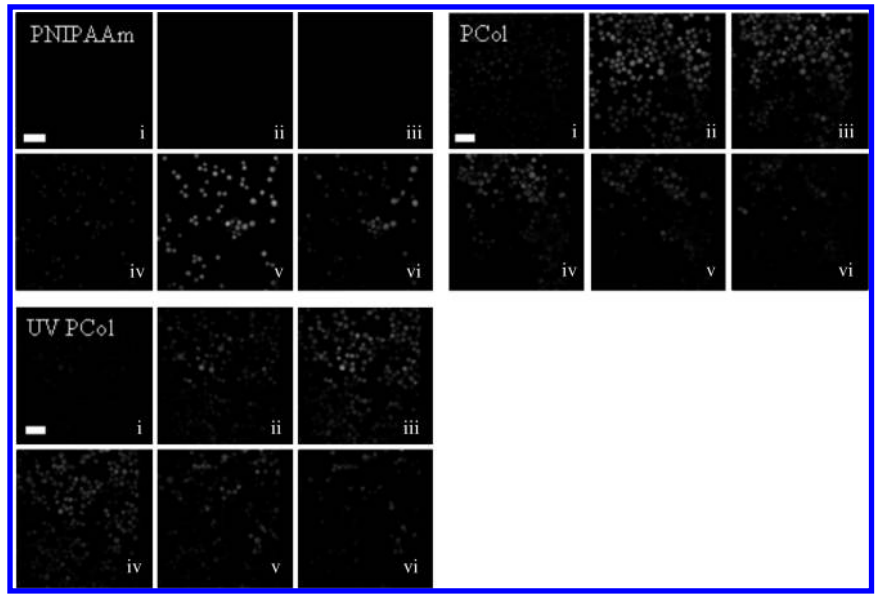

Figure 7. Confocal images of calcein-AM-stained RPE cells that have been incubated with (a) unmodified amine-terminated PNIPAAm, (b) PCol, and (c) UV PCol. Cells were incubated within the various scaffolds for 1 h prior to being placed in a 37 °C CO_2 incubator to drive scaffold formation. Images were collected using a temperature-controlled Leica DMI 6000 B confocal microscope. Z-scans show the distribution of cells from bottom to top (i−vi) for the various scaffolds. Scale bar: 80 μm.

Cellular Entrapment Within the Scaffold. In attempts to create an adequate artificial Bruch's membrane, PCol and UV PCol were synthesized with type I collagen. However, simply mixing cells together with the PCol and UV PCol scaffolds prior to gelation resulted in insufficient entrapment of RPE cells within the bulk matrix of the scaffolds, presumably due to the fact that the cells did not have time to adhere to the collagen backbone and were expelled from the bulk copolymer as the materials underwent a temperature-induced phase transition. By simply including an incubation period at room temperature prior to gelation, cell retention in the scaffolds was greatly increased. Incubation with PCol and UV PCol at temperatures below the LCST allowed RPE cells to adhere to the collagen component of the scaffold, preventing their expulsion from the bulk matrix during phase transition. Z-scans in Figure 7 show the various cell containing scaffolds at different depths from bottom to top (i−vi). Live cells were stained green with calcein AM for visualization purposes. These Z-scans demonstrate the ability of the PCol and UV PCol scaffolds to entrap cells more efficiently than unmodified PNIPAAm following gelation because cells remain dispersed throughout the cell-adhesive scaffolds but are absent in the bulk phase of the PNIPAAm gel.

The design architecture of the modified scaffolds prevents mass expulsion of cells from the biomaterial upon scaffold formation and should reduce the number of cells lost because of leakage from the injection site and anoikis. Further changes that may enhance cellular entrapment include modification of the PCol and UV PCol scaffolds to incorporate additional components of the Bruch's membrane, such as fibronectin, laminin and vitronectin, to provide a more complete approximation of the healthy Bruch's membrane. Ultimately, it may be desirable to load the scaffolds with growth factors or pharmaceuticals to help create a favorable microenvironment within the subretinal space to aid cell therapy.

Environmental Scanning Electron Microscopy. ESEM images were collected for amine-terminated PNIPAAm, unmodified collagen, PCol, and UV PCol to obtain information about the 3-D microenvironment within which transplanted cells will be entrapped. ESEM was originally utilized for the potential to view scaffolds in a hydrated state; however, the decreased pressure required for imaging rapidly dried the samples, altering their structure. Therefore, samples were swollen for 2 days at 37 °C, rapidly frozen by immersion in liquid nitrogen and lyophilized to generate a dry sample while preserving the hydrated pore structure, thereby allowing image collection via ESEM (Figure 8).

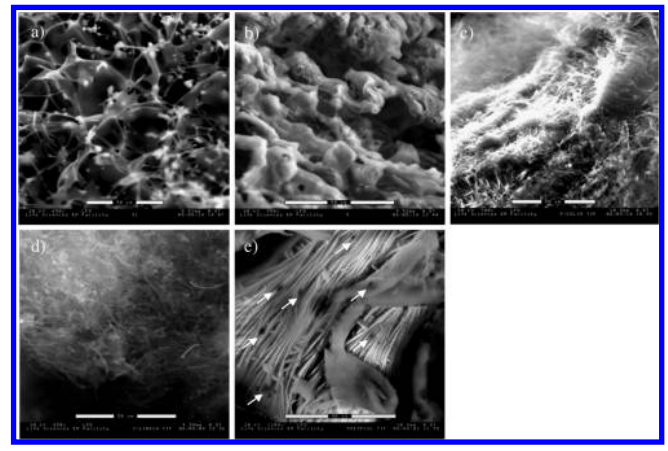

Figure 8. Environmental scanning electron microscopy images of (a) amine-terminated PNIPAAm, (b) unmodified collagen, (c) PCol, (d) UV PCol, and (e) PCol loaded with one million RPE cells. ESEM was used to image the microenvironment of the various scaffolds. Clear differences in microstructure were evident between the two synthesized scaffolds and their starting components. Scale bar: (a−d) 50 μm, (e) 40 μm.

Whereas PNIPAAm and collagen samples displayed relatively homogeneous, ordered structures, PCol and UV PCol appear highly amorphous and somewhat like a cross-linked gel. Furthermore, these materials were quite different in appearance, indicating that the chemistry of synthesis and material composition, which were different because of material processing purposes, had a strong influence on final copolymer structure. The UV PCol scaffold appears to be much more fibrillar, likely owing to a higher degree of collagen cross-linking. All scaffolds appear to be adequately porous, which is conducive to the transport of oxygen and nutrients into and out of the scaffold, allowing for nourishment of the entrapped cells, particularly over the desired times that will be necessary for the scaffolds to be present. Figure 8e shows RPE cells entrapped within the PCol scaffold; cells appear as the dark

spots within the scaffold and are indicated with white arrows. It is interesting to note the degree of variability within the PCol scaffold itself. The variability between PCol images likely stems from the use of different solvents and the presence, or absence, of cells. The PCol scaffold containing no cells was prepared in distilled water, whereas the PCol scaffold containing RPE cells was swollen in DMEM-F12 culture medium. The scaffold's environment appears to have caused changes in regional self-assembly of the copolymer during scaffold formation, resulting in a relatively amorphous structure in the presence of distilled water and highly organized, interwoven braid-like structures when swelled in cell-containing culture medium.

Conclusions

In attempts to develop a noninvasive strategy to deliver therapeutic RPE cells into the highly complex and delicate subretinal space, we decorated the backbone of type I bovine collagen with thermoresponsive PNIPAAm. Collagen was selected because it is an integral adhesion protein associated with the overall health and function of anchorage-dependent RPE cells. The incorporation of PNIPAAm was intended to decrease invasiveness of delivery by driving in situ scaffold formation via temperature-induced phase transition. Grafting of amine-terminated PNIPAAm onto the collagen backbone was achieved through either EDC/NHS chemistry (PCol) or excitation of a riboflavin photosensitizer (UV PCol). Polymer grafting was confirmed using FTIR and did not significantly alter the LCST of the scaffolds. Whereas gelling kinetics of PCol and UV PCol scaffolds were hindered slightly by the presence of bulky collagen molecules, rapid gelation was observed upon heating to body temperature. Both scaffolds displayed excellent compatibility with RPE cells, and the inclusion of a room-temperature incubation period was found to increase cellular retention drastically. The ability to support cellular engraftment of RPE cells in vitro indicates that these scaffolds may be suitable as relatively noninvasive delivery vehicles for the transplantation and support of RPE cells into the subretinal space of patients suffering from retinal degenerative diseases such as AMD and retinitis pigmentosa. Future work will examine biological response to the scaffolds including subretinal injections of RPE-carrying PCol and UV PCol biomaterials as well as the development of a degradable form of cell-adhesive PNIPAAm that will allow complete clearance from the subretinal tissues.

Acknowledgment. Funding support from NSERC is gratefully acknowledged. Photographs in Figure 4 were taken by Ron Scheffler.

Supporting Information Available. Cell viability images of RPEs cultured in the presence of PNIPAAm, PCol, and UV PCol as well as high-quality, color images of Figure 4b,c. Live cells were stained green with calcein AM, and dead cells were stained red with EthD-1. This material is available free of charge via the Internet at http://pubs.acs.org.

References and Notes

(1) Mooney, D. J.; Vandenburgh, H. Cell delivery mechanisms for tissue repair. *Cell Stem Cell* **2008**, *2*, 205–213.
(2) Nerem, R. M. Cell-based therapies: from basic biology to replacement, repair, and regeneration. *Biomaterials* **2007**, *28*, 5074–5077.
(3) MacLaren, R. E.; Pearson, R. A.; MacNeil, A.; Douglas, R. H.; Salt, T. E.; Akimoto, M.; Swaroop, A.; Sowden, J. C.; Ali, R. R. Retinal repair by transplantation of photoreceptor precursors. *Nature* **2006**, *444*, 203–207.
(4) Gouras, P.; Lopez, R.; Kjeldbye, H.; Sullivan, B.; Brittis, M. Transplantation of retinal epithelium prevents photoreceptor degeneration in the RCS rat. *Prog. Clin. Biol. Res.* **1989**, *314*, 659–671.
(5) Lane, C.; Boulton, M.; Marshall, J. Transplantation of retinal pigment epithelium using a pars plana approach. *Eye (London, U. K.)* **1989**, *3*, 27–32.
(6) Sheedlo, H. J.; Li, L.; Turner, J. E. Photoreceptor cell rescue in the RCS rat by RPE transplantation: a therapeutic approach in a model of inherited retinal dystrophy. *Prog. Clin. Biol. Res.* **1989**, *314*, 645–658.
(7) Gouras, P.; Flood, M. T.; Kjedbye, H.; Bilek, M. K.; Eggers, H. Transplantation of cultured human retinal epithelium to Bruch's membrane of the owl monkey's eye. *Curr. Eye Res.* **1985**, *4*, 253–265.
(8) Yaji, N.; Yamato, M.; Yang, J.; Okano, T.; Hori, S. Transplantation of tissue-engineered retinal pigment epithelial cell sheets in a rabbit model. *Biomaterials* **2009**, *30*, 797–803.
(9) da Cruz, L.; Chen, F. K.; Ahmado, A.; Greenwood, J.; Coffey, P. RPE transplantation and its role in retinal disease. *Prog. Retinal Eye Res.* **2007**, *26*, 598–635.
(10) Gullapalli, V. K.; Sugino, I. K.; Van Patten, Y.; Shah, S.; Zarbin, M. A. Impaired RPE survival on aged submacular human Bruch's membrane. *Exp. Eye Res.* **2005**, *80*, 235–248.
(11) Bawa, P.; Pillay, V.; Choonara, Y. E.; du Toit, L. C. Stimuli-responsive polymers and their applications in drug delivery. *Biomed. Mater.* **2009**, *4*, 22001.
(12) Monji, N.; Hoffman, A. S. A novel immunoassay system and bioseparation process based on thermal phase separating polymers. *Appl. Biochem. Biotechnol.* **1987**, *14*, 107–120.
(13) Park, T. G.; Hoffman, A. S. Effect of temperature cycling on the activity and productivity of immobilized beta-galactosidase in a thermally reversible hydrogel bead reactor. *Appl. Biochem. Biotechnol.* **1988**, *19*, 1–9.
(14) Hoare, T.; Santamaria, J.; Goya, G. F.; Irusta, S.; Lin, D.; Lau, S.; Padera, R.; Langer, R.; Kohane, D. S. A magnetically triggered composite membrane for on-demand drug delivery. *Nano Lett.* **2009**, *9*, 3651–3657.
(15) Kang Derwent, J. J.; Mieler, W. F. Thermoresponsive hydrogels as a new ocular drug delivery platform to the posterior segment of the eye. *Trans. Am. Ophthalmol. Soc.* **2008**, *106*, 206–213; discussion 213−214.
(16) Shimizu, T.; Yamato, M.; Kikuchi, A.; Okano, T. Cell sheet engineering for myocardial tissue reconstruction. *Biomaterials* **2003**, *24*, 2309–2316.
(17) Hynes, R. O. Integrins: bidirectional, allosteric signaling machines. *Cell* **2002**, *110*, 673–687.
(18) McLaughlin, B. J.; Fan, W.; Zheng, J. J.; Cai, H.; Del Priore, L. V.; Bora, N. S.; Kaplan, H. J. Novel role for a complement regulatory protein (CD46) in retinal pigment epithelial adhesion. *Invest. Ophthalmol. Visual Sci.* **2003**, *44*, 3669–3674.
(19) Imoto, Y.; Ohguro, N.; Yoshida, A.; Tsujikawa, M.; Inoue, Y.; Tano, Y. Effects of RGD peptides on cells derived from the human eye. *Jpn. J. Ophthalmol.* **2003**, *47*, 444–453.
(20) Ha, D. I.; Lee, S. B.; Chong, M. S.; Lee, Y. M. Preparation of thermoresponsive and injectable hydrogels based on hyaluronic acid and poly(*N*-isopropylacrylamide) and their drug release behaviors. *Macromol. Res.* **2006**, *14*, 87–93.
(21) Everaerts, F.; Torrianni, M.; Hendriks, M.; Feijen, J. Quantification of carboxyl groups in carbodiimide cross-linked collagen sponges. *J. Biomed. Mater. Res., Part A* **2007**, *83*, 1176–1183.
(22) van Wachem, P. B.; Plantinga, J. A.; Wissink, M. J.; Beernink, R.; Poot, A. A.; Engbers, G. H.; Beugeling, T.; van Aken, W. G.; Feijen, J.; van Luyn, M. J. In vivo biocompatibility of carbodiimide-crosslinked collagen matrices: Effects of crosslink density, heparin immobilization, and bFGF loading. *J. Biomed. Mater. Res.* **2001**, *55*, 368–378.
(23) Wollensak, G. Crosslinking treatment of progressive keratoconus: new hope. *Curr. Opin. Ophthalmol.* **2006**, *17*, 356–360.
(24) Wollensak, G.; Spoerl, E.; Seiler, T. Riboflavin/ultraviolet-A-induced collagen crosslinking for the treatment of keratoconus. *Am. J. Ophthalmol.* **2003**, *135*, 620–627.
(25) Hafezi, F.; Mrochen, M.; Iseli, H. P.; Seiler, T. Collagen crosslinking with ultraviolet-A and hypoosmolar riboflavin solution in thin corneas. *J. Cataract Refractive Surg.* **2009**, *35*, 621–624.
(26) Duan, X.; Sheardown, H. Crosslinking of collagen with dendrimers. *J. Biomed. Mater. Res., Part A* **2005**, *75*, 510–518.

BM100299J